GEOPHYSICAL RESEARCH LETTERS, VOL. 23, NO. 23, PAGES 3297-3300, NOVEMBER 15, 1996

Interferometric determination of broadband ELF wave phase velocity within a region of transverse auroral ion acceleration

J. Bonnell, P. Kintner, J.-E. Wahlund[1]
School of Electrical Engineering, Cornell University

K. Lynch, R. Arnoldy
University of New Hampshire

Abstract. Broadband electric field fluctuations with typical amplitudes of 10-20 mV/m peak-to-peak and frequencies from 0 Hz to 3 kHz (BB-ELF) were observed coincident with a region of $\leq$ 200 eV transverse H^+ acceleration (TAI) near the poleward edge of the pre-midnight aurora. The coherence and phase velocity of the electric fields were measured using a interferometric antenna array over the frequency range of $\approx$ 100 Hz to 3 kHz. These electric field fluctuations were found to have the following characteristics: 1) incoherence perpendicular to the geomagnetic field, 2) coherence parallel to the the geomagnetic field, 3) parallel phase velocity ($\omega/k_{||}$) of 30 - 35 km/s upwards, 4) $0 < |k_{||}/k_{\perp}| < 0.22$. We show that these properties are compatible with the emission being electrostatic H^+ cyclotron (EHC) waves. We also discuss possible generation mechanisms for the waves, and their relationship to the TAI.

Introduction

Using a plasma wave interferometer, we have measured the parallel phase velocity ($\omega/k_{||}$) of broadband ($\approx$ 0 Hz to 3 kHz) electric field fluctuations. Based on the oblique electric field polarization and the electrostatic nature of the emission, along with the measured phase velocity, we have identified the emission as electrostatic H^+ cyclotron (EHC) waves.

The existence of electrostatic ion cyclotron turbulence in the auroral ionosphere was predicted by *Kindel and Kennel* [1971] on the basis of the instability of H^+ and O^+ acoustic and cyclotron waves in the presence of parallel electron drift. Infrequent observations supported their conjecture. The H^+ cyclotron mode observed by *Mosier and Gurnett* [1969], and the O^+ cyclotron wave mode in the case of *Bering et al.* [1975]; *Yau et al.* [1983]; *Bering* [1984]; *Kintner et al.* [1989] were identified by the spectral characteristics of the electric field fluctuations, and the **k**-vector distribution inferred from the Doppler-shifting or -broadening of the emission. Further observations of electrostatic H^+ cyclotron waves in conjunction with TAI were made at altitudes of $1R_e$ by the S3-3 satellite [*Kintner et al.*, 1978, 1979; *Temerin et al.*, 1979; *Mozer et al.*, 1980]. These modes were identified by the presence H^+ gyrofrequency structures in the electric field spectra.

Several recent observations of BB-ELF and coincident TAI have focused on the identity of the BB-ELF and its relationship to the TAI. *Wahlund et al.* [1994b] showed that broadband electric field fluctuations observed at 1700 km in the auroral zone with $|k_{||}/k_{\perp}| > 1$ were in fact ion acoustic waves, possibly generated by the dissipation of solitary kinetic Alfvén waves [*Wahlund et al.*, 1994a]. BB-ELF coincident with TAI and large-scale density depletions was observed by *Kintner et al.* [1996] in the cleft, who concluded that the waves were current-driven and produced the TAI. *Knudsen et al.* [1996] show a strong coincidence between TAI O^+ and BB-ELF in the Freja dataset, and *Norquist et al.* [in press, 1996] have shown that resonant absorption of observed broadband electromagnetic waves can explain the observed O^+ acceleration to $\approx$20 eV. *Boehm et al.* [1995] have also reported Freja observations of TAI, low-frequency turbulence and upgoing electron beams in regions of downward $j_{||}$. There are also the EISCAT observations of ion acoustic turbulence during ion outflow and electron heating [*Rietveld et al.*, 1991; *Wahlund et al.*, 1992] which may be a related phenomenon.

Electrostatic ion cyclotron wave production of transversely accelerated ions has been theoretically investigated by many authors (for example, *Palmadesso et al.* [1974]; *Dusenbury and Lyons* [1981]; *Ashour-Abdalla and Okuda* [1984]; *Lysak* [1986]; *André and Chang* [1992]). In this paper we infer that supporting evidence exists for electrostatic ion cyclotron waves in regions of transversely accelerated ions and at the smallest plasma den-

[1]Now at IRF–Uppsala, Sweden.

Paper number 96GL03238.
0094-8534/96/96GL-03238$05.00

sities observed by sounding rockets. The AMICIST ion measurements are treated in greater detail in *Lynch et al.* [1996].

AMICIST instrumentation

AMICIST (40.007 UE) was launched from Poker Flat, Alaska, USA at 10:21:46 UT on Feb. 24, 1995 into a premidnight aurora. After the powered portion of flight, the main payload was aligned with its spin axis perpendicular to the ambient magnetic field and within 15° of the perpendicular component of the payload velocity. As shown in figure 1, the main payload carried four 1-m spherical double probe electric field antennae (2.2 cm diameter probes separated by 1 m) deployed on the end of 2.75 m booms in the spin plane of the payload. The potential between the probes of each antenna (VLF12, VLF43, VLF56, and VLF87) was bandpass-filtered to the range 10 Hz – 20 kHz, and then sampled at 40000 samples/s with 12 bit resolution. All antennae of the interferometer were sampled simultaneously. The gain of each antenna's amplifier chain was set to saturate at 417 mV/m peak-to-peak.

AMICIST data

Figure 2 shows the E field power spectrum from 10 Hz to 8 kHz for the period of 410-470s flight time. AMICIST was at an altitude of ≈ 850 km and an L-shell of 8-9 during this period. It shows the dropout of VLF hiss at 430s, the increase in broadband ELF emissions between 442-452 s, and the return of VLF hiss after 452s in the polar cap. The period of intense ELF emissions between 442-452 s is depicted in figure 3. Panel a shows the spectral density from antenna VLF87 between 10 Hz and 5 kHz. Panel b shows the count rate of ions from 6-800 eV integrated over pitch angle, and panel c shows the count rate of electrons from 0 - 16 keV (swept every 125 ms), also integrated over pitch angle. Measurements of the pitch angle spectra of ions and electrons show that the enhancements in H^+ flux are near 90° pitch angle, that of O^+ are at pitch angles $\leq 90°$, while the 1-2 s enhancements in electron flux are near 0° pitch angle. From these spectra one can see the transverse ion acceleration and enhancement in broadband ELF resolved into several bursts over the 10 s period. There are rapid changes in the ELF spectral density and ion flux which track each other at the 0.1-0.2 s level. The enhanced broadband electric field fluctuations extend from 10 Hz to ≈ 3 kHz, with the bulk of the power at low frequencies. The ELF emissions show maximum amplitude when the antenna is perpendicular to $\mathbf{B_0}$, implying that the waves have electric fields polarized mostly in the perpendicular plane. These bursts of wave emission and TAI are loosely correlated with 4 successive suprathermal electron bursts (STEB), as shown in figure 3. Perpendicular E- and B-field fluctuations of 10-50 mV/m and 10 nT ($E/B \approx 10^6$ m/s) at frequencies around 1 Hz were also observed during this event, and were most intense near the beginning (440s) and end (450s) of the event.

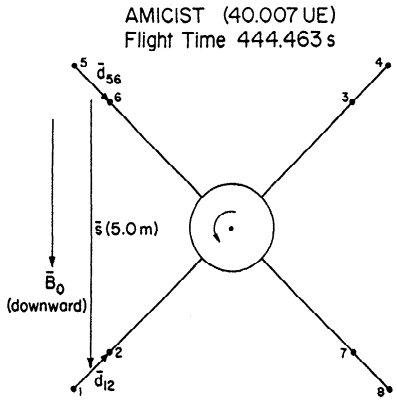

Figure 1. Schematic diagram (not to scale) of AMICIST (40.006 UE) antenna configuration and orientation with respect to $\mathbf{B_0}$ at flight time 444.463 s. The view is looking from fore to aft along the main payload, and the payload spins counter-clockwise.

We computed the cross-spectra (cf. *LaBelle and Kintner* [1989]) of all pairs of the VLF antennae, and looked for periods when these antenna pairs saw coherent signals. A persistent feature of these coherence measurements is a strong enhancement of the coherence within the frequencies of the ELF emission when the separation vector between two antennae is within 3° of parallel to $\mathbf{B_0}$. A similar increase in coherence is not seen for antennae separated perpendicularly to $\mathbf{B_0}$, nor are coherent signals observed in antennae separated across the payload (ie. VLF12 and VLF43), rather than adjacent to each other (ie. VLF12 and VLF56). Panels a) and b) of figure 4 show the phase (green) and coherence (red) of the cross spectrum between the antennae VLF12 and VLF56 (panel a) and VLF43 and VLF87 (panel b) during one of these periods. As shown in figure 1, these antenna pairs are situated on opposite sides of the main payload, with separation vectors which are oppositely directed. These cross spectra were computed using discrete 256-point Fourier transforms of the sampled data, and eight spectra were averaged to produce each cross-spectrum. Each cross-spectrum represents 51.2 ms of data.

The phase shift is given by $\phi = \mathbf{k} \cdot \mathbf{s} + \phi_0$, where $\cos\phi_0 = (\hat{\mathbf{k}} \cdot \hat{\mathbf{d}}_a)(\hat{\mathbf{k}} \cdot \hat{\mathbf{d}}_b)$, and $\mathbf{s} = \mathbf{s}_a - \mathbf{s}_b$ is parallel to $\mathbf{B_0}$ in this case, and $\mathbf{s} \cdot \mathbf{B_0} > 0$, so that $\mathbf{k} \cdot \mathbf{s} = k_{||} s$ ($k_{||} > 0$ means $k_{||}$ downward). If $\omega = 2\pi f = v k_{||}$, where v is the parallel phase velocity, then $\phi = \frac{2\pi s}{v} f + \phi_0$, showing that the slope of the phase vs. frequency trend is inversely proportional to the parallel phase velocity $\omega/k_{||}$. The obvious linear phase trend in the cross-spectra implies a constant value of $\omega/k_{||}$ below ≈3 kHz. This parallel phase velocity is typically 30-35 km/s upwards, and is consistent across the event. The measured parallel phase velocity of the emission is large compared to

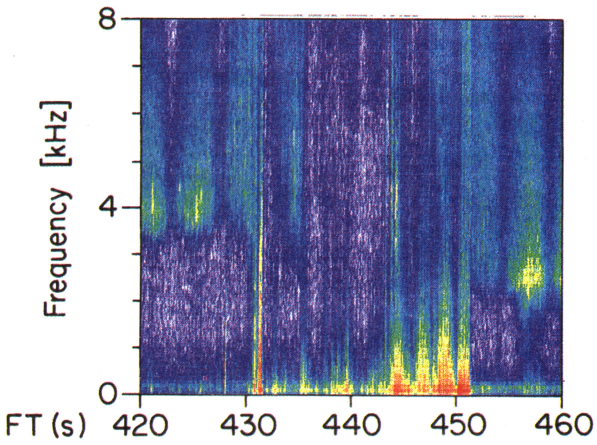

Figure 2. Survey periodogram of VLF wave data from flight times 410-470 s, over the frequency range 10 Hz to 8 kHz.

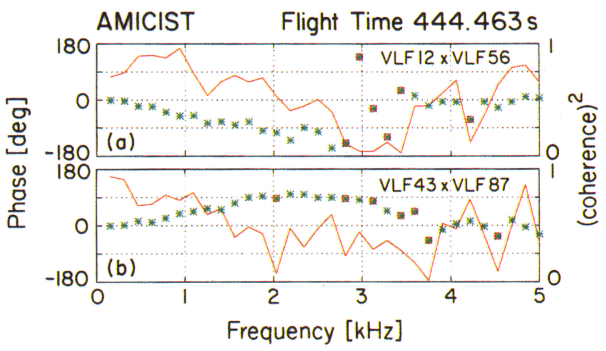

Figure 4. Cross spectral coherence and phase as a function of frequency at flight time 444.463s, showing the linear phase vs. frequency trend below 3 kHz.

the parallel velocity of the payload (0.8 km/s) relative to the Earth, and was not observed at a corresponding time during the down-leg of the flight, and so is probably not due to a "wake" effect.

If the emission were due to an isolated direction in the $\mathbf{k}_\perp$ plane, then one should see coherent signals on perpendicularly separated antennae. Such coherence is not seen, and this lack of coherence means that the waves come incoherently from many directions in the $\mathbf{k}_\perp$ plane. This can be imagined as a cone in $\mathbf{k}$-space with the $-k_{||}$ (anti-parallel) direction as its axis. The region of emission in $\mathbf{k}$-space can not lie purely in the $\mathbf{k}_\perp$ (a "pancake") plane because such a distribution of waves would have an infinite parallel phase velocity.

The spectral density at a given frequency for a conical $\mathbf{k}$-distribution is derived from the single $\mathbf{k}$-vector result (PSD $\propto (\hat{\mathbf{k}} \cdot \hat{\mathbf{d}})^2 \,\mathrm{sinc}^2(\mathbf{k} \cdot \mathbf{d}/2)$) by integrating over all directions of $\mathbf{k}_\perp$ at a fixed $|\mathbf{k}_\perp|$. This result is that PSD $\propto (1/\beta^2)(1 - \cos(k_{||}d_{||})J_0(k_\perp d_\perp))$, with $\beta = kd/2$, J_0 = 0-th order Bessel function of the 1-st kind, d = probe separation, and parallel and perpendicular are referred to $\mathbf{B_0}$. We used this result, along with

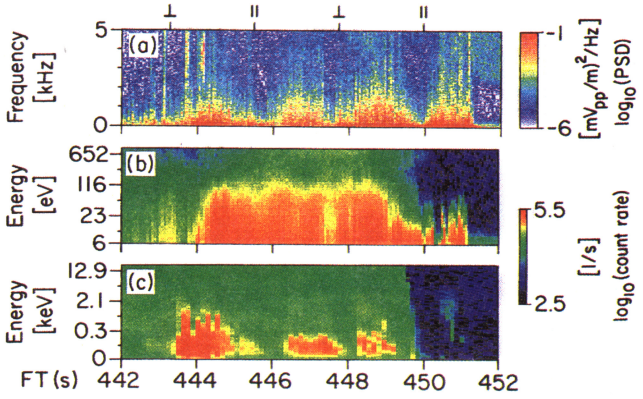

Figure 3. ELF wave and TAI event at 442-452 s. Panels described in text.

$\omega/k_{||}$ to compare the ratio of PSD measured by parallel and perpendicular antennae, which was typically $\mathrm{PSD}_\perp/\mathrm{PSD}_{||} \approx 10$. Such a ratio implies $|k_{||}/k_\perp| = 0.22$. Additional power at a given frequency which reduces the perpendicular-parallel contrast will mimic a $\mathbf{k}$-distribution with larger $|k_{||}/k_\perp|$, so this estimate is an upper limit on $|k_{||}/k_\perp|$.

There is no apparent structure in the ELF spectral density ordered by the ion gyrofrequencies (H^+, He^+, or O^+ of approx. 600 Hz, 160 Hz, and 40 Hz, respectively). The Doppler-broadening due to the motion of the payload through the plasma is $\delta f/f = 2V_p/(\omega/k_\perp) = 2V_p/((\omega/k_{||})|k_{||}/k_\perp|) \geq 0.6$, for $V_p \approx 2$ km/s, so sharp spectral features could be smeared significantly, if they exist at all.

Interpretation

We have used $\omega/k_{||}$ to look for free energy sources in the measured particle distributions and fields. None of the observed particles are in resonance with the ELF waves. An upwards drift in the thermal electrons (unmeasured) could contribute to the emission, and is consistent with the amplitude (5 μA/m^2 for V_d = 30 km/s and $n_e = 10^3$ cm^{-3}) and direction of $j_{||}$ (downwards) inferred to be carried by thermal electrons in *Fukunishi et al.* [1993], but is probably sub-threshold for the expected $T_e \geq 0.3$ eV and a drift-driven H^+ cyclotron mode [*Kindel and Kennel*, 1971]. The larger amplitude ≈ 1 Hz E and B fields could also contribute to the emission via a wave decay (wave/thermal energy density $\approx 10^{-3}$) [*Seyler et al.*, 1995] or by creating transverse shears which contribute free energy to the instability [*Ganguli and Palmadesso*, 1988]. Such shears may also explain the broadband nature of the emission [*Gavrishchaka et al.*, 1996]. Further analysis will hopefully clarify the generation mechanism.

Using the measured parallel phase velocity and propagation angle, we have computed the perpendicular phase velocity, $(\omega/k_\perp) = (\omega/k_{||})(k_{||}/k_\perp)$, using the upper limit on $|k_{||}/k_\perp|$ found above to be $\leq (0.22)(30 -$

35 km/s) = 7 – 8 km/s. The electron skin depth, $\lambda_e = c/\omega_{pe}$, is 168 m for $n_e = 10^3$ cm^{-3}, resulting in $k_\perp \lambda_e \approx 80$ at f_{cH^+}, which implys that the mode is electrostatic. For the EHC mode, $\omega/k_\perp \approx v_{tH}$, which implies a T_H of 0.3 eV, which is consistent with the lower limit on T_e and $T_e \approx T_i$.

Dusenbury and Lyons [1981] found that transverse ion heating to 10-100 times the initial perpendicular energies was possible for 10-20 mV/m peak-to-peak EHC waves with parallel phase velocities and $k_{||}/k_\perp$ similar to those observed on AMICIST, and so the observed ELF waves are a likely source for the coincident TAI.

Acknowledgments. The work of Bonnell, Kintner, and Wahlund was supported by NASA grant NAG 5-5008. The work of Lynch and Arnoldy was supported by NASA grant NAGW 5007.

References

André, M., and T. Chang, Ion heating perpendicular to the magnetic field, in *Physics of Space Plasmas (1992), SPI Conference Proceedings and Reprint Series, Number 12*, 1992.

Ashour-Abdalla, M., and H. Okuda, Turbulent heating of heavy ions on auroral field lines, *J. Geophys. Res.*, *89*, 2235, 1984.

Bering, E. A., The plasma wave environment of an auroral arc: electrostatic ion cyclotron waves in the diffuse aurora, *J. Geophys. Res.*, *89*, 1635, 1984.

Bering, E. A., et al., Observations of an intense field-aligned thermal ion flow and associated intense narrow band electric field oscillations, *J. Geophys. Res.*, *80*, 4612, 1975.

Boehm, M. H., et al., Observations of an upward-directed electron beam with the perpendicular temperature of the cold ionosphere, *Geophys. Res. Lett.*, *22*, 2103, 1995.

Dusenbury, P. B., and L. R. Lyons, Generation of ion-conic distributions by upgoing ionospheric electrons, *J. Geophys. Res.*, *86*, 7627, 1981.

Fukunishi, H., et al., Latitudinal structures of nightside field-aligned currents and their relationships to plasma sheet regions, *J. Geophys. Res.*, *98*, 11235, 1993.

Ganguli, G., and P. Palmadesso, Electrostatic ion instabilities in the presence of parallel currents and transverse electric fields, *Geophys. Res. Lett.*, *15*, 103, 1988.

Gavrishchaka, V., et al., Dispersive properties of a magnetized plasma with a field-aligned drift and inhomgeneous transverse flow, *Phys. of Plasmas, in press*, 1996.

Kindel, J. M., and C. F. Kennel, Topside current instabilities, *J. Geophys. Res.*, *76*, 3055, 1971.

Kintner, P. M., et al., Electrostatic hydrogen cyclotron waves near one Earth radius altitude in the polar magnetosphere, *Geophys. Res. Lett.*, *5*, 139, 1978.

Kintner, P. M., et al., Simultaneous observations of energetic (keV) upstreaming and electrostatic hydrogen cyclotron waves, *J. Geophys. Res.*, *84*, 7201, 1979.

Kintner, P. M., et al., Simutaneous observations of electrostatic oxygen cyclotron waves and ion conics, *Geophys. Res. Lett.*, *16*, 739, 1989.

Kintner, P. M., et al., SCIFER – transverse ion acceleration and plasma waves, *Geophys. Res. Lett.*, *23*, 1873, 1996.

Knudsen, D. J., et al., Correlation between core ion energization, suprathermal electron bursts, and broad-band ELF plasma waves, *J. Geophys. Res., in press*, 1996.

LaBelle, J., and P. M. Kintner, The measurement of wavelength in space plasmas, *Rev. Geophys.*, *27*, 495, 1989.

Lynch, K. R., et al., The AMICIST sounding rocket – a comparison of transverse ion acceleration mechanisms, *Geophys. Res. Lett., in press*, 1996.

Lysak, R. L., Ion acceleration by wave-particle interaction, in *Ion acceleration in the magnetosphere and ionosphere*, edited by T. Chang, Washington, D. C., American Geophysical Union, 1986.

Mosier, S. R., and D. A. Gurnett, Ionospheric observation of VLF electrostatic noise related to harmonics of the proton gyrofrequency, *Nature*, *223*, 605, 1969.

Mozer, F. S., et al., Satellite measurements and theories of low altitude aurora particle acceleration, *Space Sci. Rev.*, *27*, 155, 1980.

Norquist, P., et al., Ion cyclotron heating in the dayside magnetosphere, *J. Geophys. Res.*, in press, 1996.

Palmadesso, P. J., et al., Topside ionosphere heating due to electrostatic ion cyclotron turbulence, *Geophys. Res. Lett.*, *1*, 105, 1974.

Rietveld, M. T., et al., Naturally enhanced ion acoustic waves in the auroral ionosphere observed with the EISCAT 933-MHz radar, *J. Geophys. Res.*, *96*, 19291, 1991.

Seyler, C. E., et al., Theory and simulation of low frequency plasma waves and comparison to Freja observations, *J. Geophys. Res.*, *100*, 21453, 1995.

Temerin, M., et al., Nonlinear steepening of the electrostatic ion cyclotron wave, *Phys. Rev. Letters*, *43*, 1941, 1979.

Wahlund, J.-E., et al., EISCAT observations of topside ionospheric ion outflows during auroral activity: revisted, *J. Geophys. Res.*, *97*, 3019, 1992.

Wahlund, J.-E., et al., On ion acoustic turbulence and the nonlinear evolution of kinetic Alfvén waves in the aurora, *Geophys. Res. Lett.*, *21*, 1831, 1994a.

Wahlund, J.-E., et al., Observations of ion acoustic fluctuations in the auroral topside ionosphere by the FREJA S/C, *Geophys. Res. Lett.*, *21*, 1835, 1994b.

Yau, A. W., et al., Particle and wave observations of the low-altitude ionospheric acceleration events, *J. Geophys. Res.*, *88*, 341, 1983.

J. Bonnell and P. Kintner, 304 Rhodes Hall, Cornell University, Ithaca, NY 14850 (johnb@ee.cornell.edu, paul@ee.cornell.edu)

K. Lynch and R. Arnoldy, Institute for the Study of Earth, Oceans, and Space, University of New Hampshire, Durham, NH (lynch@unhedi1.sr.unh.edu, arnoldy@unhedi1.sr.unh.edu)

J.-E. Wahlund, Swedish Institute of Space Physics, Uppsala Division, Uppsala, Sweden (jwe@irfu.se)

(received June 4, 1996; revised August 16, 1996; accepted August 28, 1996.)